Inactivation of N-type Calcium Current in Chick Sensory Neurons: Calcium and Voltage Dependence

DANIEL H. COX and KATHLEEN DUNLAP

From the Departments of Physiology and Neuroscience, Tufts University School of Medicine, Boston, Massachusetts 02111

ABSTRACT We have studied the inactivation of high-voltage-activated (HVA), ω-conotoxin-sensitive, N-type Ca^{2+} current in embryonic chick dorsal root ganglion (DRG) neurons. Voltage steps from −80 to 0 mV produced inward Ca^{2+} currents that inactivated in a biphasic manner and were fit well with the sum of two exponentials (with time constants of ~100 ms and >1 s). As reported previously, upon depolarization of the holding potential to −40 mV, N current amplitude was significantly reduced and the rapid phase of inactivation all but eliminated (Nowycky, M. C., A. P. Fox, and R. W. Tsien. 1985. *Nature.* 316:440–443; Fox, A. P., M. C. Nowycky, and R. W. Tsien. 1987*a*. *Journal of Physiology.* 394:149–172; Swandulla, D., and C. M. Armstrong. 1988. *Journal of General Physiology.* 92:197–218; Plummer, M. R., D. E. Logothetis, and P. Hess. 1989. *Neuron.* 2:1453–1463; Regan, L. J., D. W. Sah, and B. P. Bean. 1991. *Neuron.* 6:269–280; Cox, D. H., and K. Dunlap. 1992. *Journal of Neuroscience.* 12:906–914). Such kinetic properties might be explained by a model in which N channels inactivate by both fast and slow voltage-dependent processes. Alternatively, kinetic models of Ca-dependent inactivation suggest that the biphasic kinetics and holding-potential-dependence of N current inactivation could be due to a combination of Ca-dependent and slow voltage-dependent inactivation mechanisms. To distinguish between these possibilities we have performed several experiments to test for the presence of Ca-dependent inactivation. Three lines of evidence suggest that N channels inactivate in a Ca-dependent manner. (*a*) The total extent of inactivation increased 50%, and the ratio of rapid to slow inactivation increased ~twofold when the concentration of the Ca^{2+} buffer, EGTA, in the patch pipette was reduced from 10 to 0.1 mM. (*b*) With low intracellular EGTA concentrations (0.1 mM), the ratio of rapid to slow inactivation was additionally increased when the extracellular Ca^{2+} concentration was raised from 0.5 to 5 mM. (*c*) Substituting Na^+ for Ca^{2+} as the permeant ion eliminated the rapid phase of inactivation. Other results do not support the notion of current-dependent inactivation, however. Although high intracellular EGTA (10

Address correspondence to Kathleen Dunlap, Department of Physiology, Tufts University School of Medicine, 136 Harrison Avenue, Boston, MA 02111.

Daniel Cox's present address is Department of Molecular and Cellular Physiology, Howard Hughes Medical Institute, Beckman Center, Stanford University, Stanford, CA 94305-5426.

J. GEN. PHYSIOL. © The Rockefeller University Press · 0022-1295/94/08/0311/26 $2.00 311
Volume 104 August 1994 311–336

mM) or BAPTA (5 mM) concentrations suppressed the rapid phase inactivation, they did not eliminate it. Increasing the extracellular Ca^{2+} from 0.5 to 5 mM had little effect on this residual fast inactivation, indicating that it is not appreciably sensitive to Ca^{2+} influx under these conditions. Thus, it appears that both voltage- and current-dependent mechanisms underlie N current inactivation in chick sensory neurons, the latter only becoming significant under low Ca^{2+}-buffering conditions.

INTRODUCTION

Voltage-activated Ca^{2+} channels provide a link between electrical activity and intracellular chemical signaling. They are believed to play a crucial role in a number of cellular processes including regulation of gene expression, excitation-contraction coupling and neurotransmitter release (Sheng, McFadden, and Greenberg, 1990; Catterall, 1991; Augustine, Charlton, and Smith, 1987). Over the last few years, high-voltage-activated (HVA) Ca^{2+} channels have been classified into N, L, and P types based on their sensitivity to various pharmacological agents (Swandulla, Carbone, and Lux, 1991; Llinas, Sugimori, Hillman, and Cherksey, 1992).

When studied from a holding potential of −80 mV, the HVA Ca^{2+} current of chick dorsal root ganglion (DRG) neurons inactivates with both fast and slow components. In general, the fast component has a time constant of ~100 ms, and the slow component decays with a time constant greater than 1 s (Nowycky, Fox, and Tsien, 1985; Fox, Nowycky, and Tsien, 1987*a;* Swandulla and Armstrong, 1988). Interestingly, when the holding potential is depolarized from −80 to −40 mV, the peak Ca^{2+} current amplitude is reduced, and the rapid phase of inactivation is nearly eliminated. These observations were explained early on by single channel recordings in DRG cells that revealed noninactivating, DHP-sensitive, L-type channels whose activity was undiminished by changes in holding potential, and inactivating, DHP-resistant, N-type channels that were sensitive to changes in holding potential (Fox, Nowycky, and Tsien, 1987*b*). Such observations prompted these investigators to classify the rapidly inactivating component of Ca^{2+} current as N-type, and the slow component as L-type (Nowycky et al., 1985; Fox et al., 1987*a,b*). More recent experiments, however, have demonstrated that most of the HVA Ca^{2+} current in chick DRG neurons is blocked by ω-conotoxin (ω-CgTx), a peptide toxin from the marine snail *Conus geographus,* which does not block L or P-type currents (Aosaki and Kasai, 1989; Plummer, Logothetis, and Hess, 1989; Regan, Sah, and Bean, 1991). In fact, in chick DRG cells less than 1 d in vitro, all of the HVA Ca^{2+} current is blocked by ω-CgTx and thus defined as N-type (Cox and Dunlap, 1992). In light of this result, it becomes clear that the properties of HVA Ca^{2+} current inactivation listed above, which were originally attributed to a combination of L and N current, are associated solely with N current.

A wide variety of presynaptic inhibitory transmitters including: norepinephrine (NE), GABA, adenosine, opioids and LHRH have been shown to modulate the response of N-type channels to changes in membrane potential (Dunlap and Fischbach, 1978, 1981; Forscher and Oxford, 1985; Kasai and Aosaki, 1989; Plummer et al., 1989; Elmslie, Zhou, and Jones, 1990; Sah, 1990; Regan et al., 1991; Cox and Dunlap, 1992; Boland and Bean, 1993). This is perhaps not surprising in view of the fact that N channels trigger neurotransmitter release at a variety of central

and peripheral synapses (Kerr and Yoshikami, 1984; Hirning, Fox, McCleskey, Olivera, Thayer, Miller, and Tsien, 1988; Holz, Dunlap, and Kream, 1988; Lipscombe, Kongsamut, and Tsien, 1989; Horne and Kemp, 1991; Gruner, Silva, and Dunlap, 1992). Alterations in N channel function may, therefore, modulate neurotransmitter release (Hirning et al., 1988; Holz et al., 1988; Lipscombe et al., 1989). Another potentially important mechanism for N channel modulation, and thus, the regulation of neurotransmission, is the inactivation of these channels produced by sustained depolarizations (Frank and Fourtes, 1957; Eide, Jurna, Jansen, and Lunberg, 1968). An understanding of the properties and underlying mechanism of this process will be essential in order to ascertain the effects of N channel inactivation on neurotransmission. A better understanding of the inactivation process may also facilitate the identification of calcium channel currents observed at the single channel level which contribute to macroscopic N current.

Mechanisms of Ca^{2+} current inactivation can be divided into two categories: (*a*) voltage-dependent inactivation (as originally described by Hodgkin and Huxley (1952) for the squid giant axon Na^+ channel) involves transitions of channel molecules into a refractory state that is promoted by depolarization. (*b*) Ca^{2+}-dependent inactivation (as originally described by Brehm and Eckert [1978] and Tillotson [1979]) involves transitions of channel molecules into a refractory state that is produced by binding of Ca^{2+} ions following their influx through open channels. HVA Ca^{2+} current of molluscan neurons exhibits biphasic inactivation kinetics qualitatively similar to that of N current in chick DRG neurons. The biphasic nature of inactivation in these neurons is most likely due to Ca^{2+}-dependent inactivation of a single current type (Chad, Eckert, and Ewald, 1984; Eckert and Chad, 1984).

The similarity in inactivation kinetics of Ca^{2+} current in molluscan and chick DRG neurons has prompted us to test the hypothesis that the N current in these cells inactivates in a Ca^{2+}-dependent manner. We report here the results of several experiments which suggest that the N channels of chick DRG neurons can inactivate by a Ca-dependent process; however, the biphasic kinetics of inactivation observed with high concentrations of Ca^{2+} chelators in the patch pipette are predominately due to voltage-dependent processes.

METHODS

Culture

Dorsal root ganglia were dissected from 11–12 d chicken embryos, dissociated by trituration and grown in cell culture according to methods previously described (Holz et al., 1988). Recordings were made from DRG neurons within 24 h of plating. At this stage in culture, neurons exhibited only short, thin processes or none at all and good spatial control of voltage could be attained.

Electrical Recording

All experiments were performed using standard tight-seal, whole cell recording techniques (Hamill, Marty, Neher, Sakmann, and Sigworth, 1981) with a List EPC-7 patch-clamp amplifier. Capacity transients were compensated using the EPC-7's cancellation circuitry, and series resistance (typically 3–4 MΩ) was compensated to ~50%. Cells were routinely stimulated

every 10 s except during the generation of *I–V* and steady state activation curves, during which test pulses were given every 2 s. Current traces were digitized at 10 KHz and digitally filtered at 1 KHz for display. Some data analysis was done with "Igor" graphing and analysis software from WaveMetrics (Lake Oswego, OR) on a Macintosh computer. High-voltage-activated (HVA) Ca^{2+} currents from all cells studied were completely blocked by 5 μM ω-conotoxin GVIA (ω-CgTx). Capacity and leak currents were routinely subtracted from Ca^{2+} currents by subtracting traces taken after ω-CgTx block from those taken before, as indicated in the figure legends. Currents carried by monovalent ions through Ca^{2+} channels were not always completely blocked by ω-CgTx. Capacity and leak currents were either left unsubtracted from these traces, or subtracted using a standard P/4 protocol with a holding potential of −120 mV as indicated in the figure legends. Tail current amplitudes were measured at the apparent peak of the tail current from unfiltered P/4 subtracted records. The amplitudes of the fast and slow components of inactivation were determined from the amplitudes of the two exponential functions used to fit each trace.

Solutions/Chemicals

ω-CgTx GVIA was obtained from Bachem California (Torrance, CA), stored as a 1 mM stock solution in distilled water, and diluted to 5 μM in external recording solution the day of the experiment. ω-CgTx was applied, and external solutions were exchanged, by superfusion from puffer pipettes with tip diameters approximately 3–5 μm as previously described (Rane and Dunlap, 1990).

For most experiments the following solutions were used. Variations in these solutions are indicated, when necessary, in the figure legends. Patch pipettes were filled with (in millimolar) CsOH 188, Gluconic acid 112, ethyleneglycol-bis-(b-amino-ethyl ether) *N,N'*-tetraacetic acid (EGTA) 10 unless indicated as 0.1, Hepes 10, NaCl 3.6 (pH = 7.4). Ca^{2+} current measurements were made with the following external solution (in mM): Na-glutamate 79, glutamic acid 70, TEA-OH 50, Hepes 25, CsOH 8.3, glucose 5, $CaCl_2$ 1, $MgCl_2$ 0.8, tetrodotoxin (TTx) 3 μM (pH = 7.4). Na^+ currents through Ca^{2+} channels were recorded with the following external solution: glutamic acid 143, TEA-OH 110, Hepes 25, CsOH 8.3, glucose 5, NaOH 28, NaCl 3.6, EGTA 1, TTx 3 μM (pH = 7.4).

RESULTS

Isolation of N Current

We have studied the kinetics of Ca^{2+} current inactivation in chick DRG neurons. Our study was limited to neurons that had been in culture less than 24 h. At this stage, DRG neurons had extended only short, thin processes (or none at all), and good spatial control of voltage could be attained. Few cells (<10%) exhibited low voltage-activated (LVA) Ca^{2+} current as judged by a lack of inward current upon depolarization to −40 mV, and the absence of a transient, ω-CgTx-resistant current. Those cells which clearly displayed LVA Ca^{2+} current were excluded from our analysis. In all cells examined (n = 69), all HVA inward current was irreversibly blocked by ω-CgTx (Fig. 1 *A*), a toxin which has been used to separate N-type from L-type Ca^{2+} currents in several cell types (Aosaki and Kasai, 1989; Plummer et al., 1989; Regan et al., 1991; Cox and Dunlap, 1992). Taking advantage of the toxin's specificity, we routinely subtracted capacity and leak currents from the Ca^{2+} current records by subtracting traces taken after from those taken before ω-CgTx (5 μM)

application. This procedure also insured that there were no voltage-dependent, ω-CgTx-resistant currents which might otherwise have contaminated our records.

Care was also taken to eliminate Ca^{2+}-activated Cl^- current (Cl_{Ca}^-) from Ca^{2+} current records (Mayer, 1985; Bernheim, Bader, Bertrand, and Schlichter, 1989). In solutions in which Cl^- was the major internal and external anion, prolonged (1 s) depolarizations stimulated sufficient Ca^{2+} entry to evoke Cl_{Ca}^- current. Such current was observed after repolarizations as a prolonged tail current sometimes lasting hundreds of milliseconds. To minimize Cl_{Ca}^- current, the internal and external Cl^- concentrations were reduced to 3.6 mM. This effectively eliminated Cl_{Ca}^- current

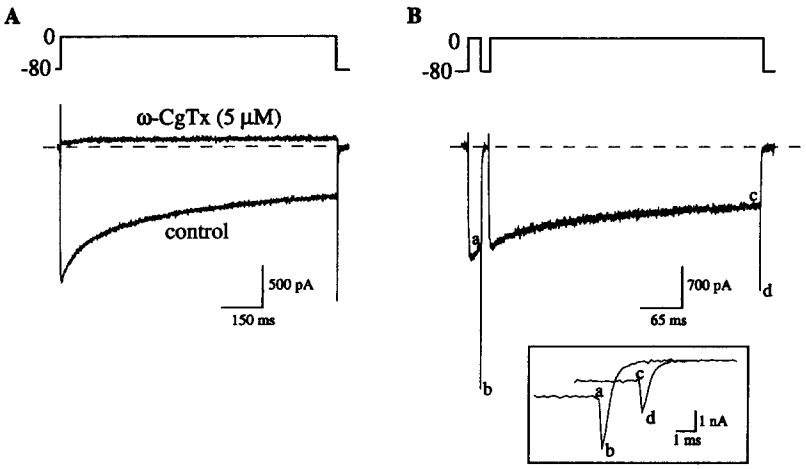

FIGURE 1. Isolation of N-type Ca^{2+} current. (*A*) Whole cell currents recorded from a chick DRG neuron during 1 s depolarizations from −80 to 0 mV before (*control*) and 1 min after superfusion of the cell with 5 μM ω-CgTx. (*B*) Cell was subjected to a voltage protocol consisting of two depolarizing test pulses from −80 to 0 mV, the first 20 ms and the second 400 ms in duration. The two pulses were separated by a 10-ms pulse to −80 mV. Capacity and leak currents were subtracted from each trace with a P/4 protocol. Peak tail current amplitudes were measured after repolarization from each test pulse (points *b* and *d*). The ratio of these amplitudes was compared to the ratio of current amplitudes measured just before repolarization (points *a* and *c*). (*Inset*) Tail currents on an expanded time scale. 10 mM EGTA was included in the patch pipette for each experiment. In this and subsequent figures, horizontal dashed lines represent zero current.

when 10 mM EGTA was included in the patch pipette solution. As discussed later, some experiments were performed with 0.1 mM EGTA in the patch pipette. Under these conditions, a larger percentage (~50%) of cells displayed Cl_{Ca}^- currents. As this current is expected to be largest at repolarized potentials away from 0 mV, only cells which showed little or no prolonged current after repolarization to −80 mV, and were thus not contaminated with Cl_{Ca}^- current, were included in our study.

To test whether contaminating outward Cs^+ current contributed to the time course of DRG neuron Ca^{2+} currents, we studied tail currents at the Cs^+ equilibrium potential (set to −80 mV). Using the two-pulse protocol illustrated in Fig. 1 *B*, tail

currents were measured at two points in time after the initial depolarization, 20 ms (near peak Ca^{2+} current) and 430 ms (after substantial decline in net inward current). The decline in tail current amplitude matched precisely (within 2%) the decline in net inward current measured at 0 mV during the interval between these time points (n = 9), indicating that the decay in Ca^{2+} current results from Ca^{2+} channel inactivation rather than the activation of a contaminating outward current. Consistent with this, the Ca^{2+}-activated K^+ channel antagonist charybdotoxin (at 50 nM) was without effect on the Ca^{2+} current (data not shown).

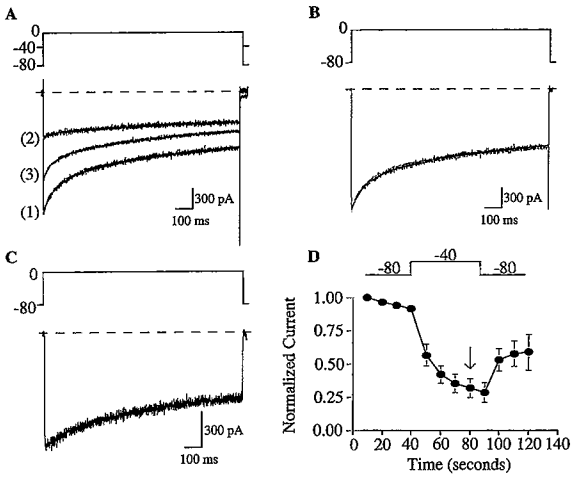

FIGURE 2. Biphasic kinetics of N current inactivation. (*A*) Whole cell Ca^{2+} currents measured during 1-s voltage steps to 0 mV from either a −80 (*1*), (*3*), or a −40 mV (*2*) holding potential (V_h). Trace *2* was recorded 40 s after the change in V_h. Trace *3* was recorded 60 s after moving the holding potential back to −80 mV. (*B*) Trace *1* of (*A*) was fit with the sum of two exponential functions (*white line*) with amplitudes of −735 and −1510 pA, and time constants of 81 and 2,720 ms, respectively. (*C*) Ca^{2+} current recorded from a different cell under the same conditions as trace 1 in (*A*), demonstrating a cell with an unusually small rapid component of inactivation. (*D*) Plotted time course of the change in current amplitude after V_h depolarization from −80 to −40 mV. Each filled circle represents the mean of five experiments. Error bars represent standard deviation from the mean. For quantitation of the change in current amplitude with V_h, peak current measurements were made before and 40 s after (*arrow*), depolarization of the holding potential from −80 to −40 mV. 10 mM EGTA was included in the patch pipette for each experiment. Current traces recorded after N current block with 5 μM ω-CgTx were used for leakage subtraction.

Properties of N Current Inactivation

Having established that the inactivation we observed was due only to HVA Ca^{2+} channels, we proceeded to characterize this process. In Fig. 2 *A* (trace *1*) is displayed a Ca^{2+} current recorded during a voltage step from −80 to 0 mV. The pipette solution contained 10 mM EGTA. Over the course of this 1-s depolarization, the current inactivated in a biphasic manner to 46% of its peak value. In 18 similar experiments, the Ca^{2+} current inactivated to 70 ± 6.3% of its peak value in 200 ms and to 46 ± 9.8% of its peak in 1 s (averages ± SD). The inactivation process could be fit well with the sum of two exponentials as shown in Fig. 2 *B*. The mean time constant for the fast component of inactivation was 102 ± 23 ms, whereas the slow component had a time constant which was greater than 2,000 ms. In general, the

amplitude of the fast component was ~0.5 that of the slow component, and this ratio varied little over recording times up to 30 min. In 20% of cells studied, currents showing relatively little fast inactivation were observed. An extreme example of this is shown in Fig. 2 *C*.

The peak amplitude and inactivation kinetics of N-type Ca^{2+} current are dependent on holding potential (Nowycky et al., 1985; Fox et al., 1987*a;* Swandulla and Armstrong, 1988; Aosaki and Kasai, 1989; Plummer et al., 1989; Regan et al., 1991; Cox and Dunlap, 1992). The currents in Fig. 2 *A* were measured following step depolarizations to 0 mV from a holding potential of −80 mV (trace *1*) or 40 s after the holding potential was shifted from −80 to −40 mV (trace *2*). On average, peak Ca^{2+} current was reduced 57 ± 12% (n = 10) by this manipulation. In addition, the rapid phase of inactivation was preferentially diminished at less negative holding potentials; in 10 cells, the currents elicited from −40 mV exhibited predominately the slow component of inactivation (inactivating to 86 ± 7.5% of its peak amplitude in 200 ms and to 65 ± 15% of peak in 1 s). The decline in current amplitude with depolarization of the holding potential developed over tens of seconds, and, as can be seen in Fig. 2 *D*, was nearly complete at 40 s. This time point was chosen for comparison because at times later than 40 s the slow decline in current amplitude was sometimes difficult to distinguish from current run-down. The process by which the N current amplitude inactivates when the holding potential is shifted from −80 to −40 mV must be strictly voltage-dependent, as no inward current is produced by this depolarization. Return of the holding potential to −80 mV reverses the inactivation (Fig. 2 *A*, trace *3*), distinguishing this voltage-dependent decline in inward current from run-down. No rapid alterations in the ratio of fast to slow inactivation were observed in our recordings over time, again arguing against the selective run-down of one of the two components.

As with the N current described here, the HVA Ca^{2+} current of molluscan neurons inactivates with both fast and slow components (Chad et al., 1984; Eckert and Chad, 1984). Chad, Eckert and colleagues (Brehm and Eckert, 1978; Tillotson, 1979; Chad et al., 1984; Eckert and Chad, 1984) have demonstrated that the biphasic inactivation of this current is due to a Ca^{2+}-dependent process. They have further shown that the ratio of the rapid to slow phase of inactivation is reduced when the current is partially block with Cd^{2+} (Chad et al., 1984). Mathematical models of Ca-dependent inactivation suggest that this effect is due to a decrease in the initial rate of Ca^{2+} accumulation near the inner surface of the channels as the maximum rate of Ca^{2+} entry is reduced (Eckert and Chad, 1984). As described above, with the N current of chick DRG neurons we see a similar reduction in the rapid phase of inactivation as the current amplitude is reduced in this case by depolarizing the holding potential from −80 to −40 mV. These results raise the possibility that the biphasic inactivation we observe over the course of 1-s depolarizations from −80 to 0 mV is predominately due to a current-dependent process. The kinetics of this process might then be altered by changes in current amplitude such as is brought about the slower voltage-dependent inactivation observed upon depolarizing the holding potential from −80 to −40 mV (Fig. 2 *D*). Alternatively, the properties of N current inactivation might be explained by a combination of fast and slow voltage-dependent processes. If the fast inactivation process is incomplete such that at −40 mV a near

maximal amount of inactivation is achieved, further depolarization to 0 mV would results in a current of smaller amplitude whose decay was due only to slow, voltage-dependent inactivation thus accounting for the loss of the rapid phase of inactivation upon depolarization of the holding potential. To distinguish between these two possibilities we looked for evidence of Ca dependence to the N current inactivation.

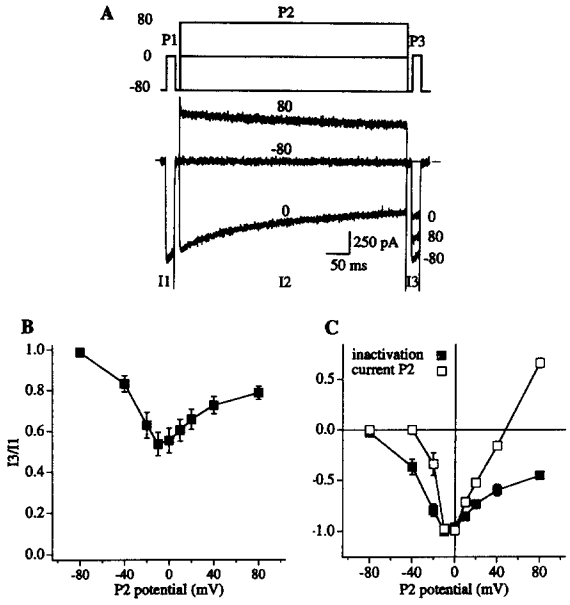

FIGURE 3. Comparison of N current inactivation rate with Ca^{2+} entry. Whole cell Ca^{2+} currents were measured during three successive depolarizing voltage pulses separated by 10-ms intervals. Holding potential was −80 mV. The first (*P1*) and third (*P3*) pulses were each to 0 mV for 20 ms. The second pulse (*P2*) was 500 ms long and variable in amplitude. Stimuli were delivered at 0.1 Hz. The amplitudes of *P2* were delivered in the following order: (−80, +80, 0, −40, +40, −20, +20, 0, −10, and +10). The ratio of the peak current during *P3* to that of *P1* (*I3/I1*) was used as an index of the inactivation occurring during *P2*. (*A*) Displays currents recorded with *P2* at −80, +80, and 0 mV. Current traces recorded after N current block with 5 μM ω-CgTx were used for leakage subtraction. 10 mM EGTA was present in the patch pipette for each experiment. (*B*) Plotted *I3/I1* as a function of *P2* potential. Plotted points represent the mean ± SD of six experiments. In *C*, the data of *B* have been normalized to maximal inactivation and plotted as a function of voltage together with the normalized mean current ($I2/I2_{max}$).

Inactivation as a Function of Prepulse Potential

We first compared Ca^{2+} influx and inactivation. The experiment of Fig. 3 employs a variation on the classic two-pulse protocol used by previous investigators to test for the presence of current-dependent inactivation (Brehm and Eckert, 1978; Eckert and Chad, 1984; Kalman, O'Lague, Erxleben, and Armstrong, 1988; Kasai and Aosaki, 1988). In this experiment, a conditioning prepulse of varying amplitude and fixed duration is followed by a short test pulse to a potential that evokes maximal current. The amplitude of the current during the test pulse is used as an indicator of the extent of inactivation produced by the prepulse. If the inactivation during the prepulse is strictly current-dependent, maximum inactivation should occur at the potential which elicits maximum inward current.

We used a three-pulse protocol with test pulses to 0 mV before and after a 500-ms conditioning pulse. The current amplitude evoked by pulse 3 (I_3) divided by that evoked by pulse 1 (I_1) was then plotted as a function of the conditioning potential (Fig. 3 *B*). When this curve is compared with the mean current produced by each conditioning pulse (Fig. 3 *C*), it is clear that maximum inactivation occurs at the point of peak current and decreases at both more negative and more positive potentials. (Note that the time base in Fig. 3 is expanded relative to that in Fig. 2, making the rapidly inactivating component less apparent to the eye.) In addition to this apparent current-dependent inactivation, substantial inactivation (~20%) is produced by prepulses to −40 mV where no measurable inward current is observed. This is as expected if we are observing a combination of slow, voltage-dependent and current-dependent inactivation processes. It has been demonstrated, however, that such a U-shaped inactivation curve can be explained by a strictly voltage-dependent model of inactivation in which the microscopic rate constant for inactivation decreases rather than increases with more positive depolarizations (Jones and Marks, 1989). These results, therefore, do not provide conclusive evidence for current dependence.

Inactivation as a Function of the Intracellular Ca^+ Buffer Concentration

If a Ca^{2+}-dependent inactivation process exists in these cells, and the site of Ca^{2+} action is accessible to intracellular Ca^{2+} buffers, one would expect that as the concentration of buffer is reduced, the initial rate and the extent of inactivation should increase. Such effects were observed for the N current of chick DRG neurons. Fig. 4 illustrates the change in the inactivation kinetics produced upon lowering the concentration of EGTA in the patch pipette from 10 to 0.1 mM. The traces in the upper and middle panels are typical of currents recorded from different cells in the presence of each concentration of EGTA. When the currents are normalized and superimposed (as shown in the lower panel of Fig. 4), it becomes clear that the current measured with 0.1 mM internal EGTA inactivates to a greater extent than that with 10 mM internal EGTA. Comparing many cells, the N current inactivated to 70 ± 6.3% of peak in 200 ms and to 46 ± 9.8% in 1 s for 10 mM EGTA (n = 18) as compared to 52 ± 8.6% of peak in 200 ms and 20 ± 7.2% in 1 s for 0.1 mM EGTA [n = 14]). In Fig. 4 (*middle*), two traces are superimposed. The more lightly colored trace was recorded 6 s after the darker trace demonstrating that the increased inactivation observed with 0.1 mM EGTA in the patch pipette recovered within seconds when the membrane potential was returned to −80 mV. The two-pulse experiment of Fig. 1 *B* was also performed during recordings with 0.1 mM internal EGTA. Again no significant difference (within 2%, n = 6) between the decline in tail current amplitude measured at −80 mV and the inactivation of the test pulse current measured at 0 mV was observed, indicating that the more prominent rapid phase of inactivation observed in the low EGTA condition was not due to the development of a Ca^{2+}-dependent outward current (data not shown). At both EGTA concentrations, the kinetics of inactivation were biphasic, and the fast time constants were indistinguishable (100 ± 23 ms with 0.1 mM EGTA and 102 ± 23 ms with 10 mM EGTA). The slow time constants could not be accurately measured with 1-s depolarizations; however, in general, it appeared that at 0.1 mM EGTA the slow time constant was

between 1 and 2 seconds, while at 10 mM EGTA it was greater than 2 s. The mean ratio of the amplitude of the fast phase of inactivation relative to the slow phase (A_{fast}/A_{slow}) increased from 0.45 to 0.98 when the concentration of EGTA in the patch pipette was lowered. These results are consistent with the presence of a Ca^{2+}-dependent inactivation mechanism.

Inactivation as a Function of the Extracellular Ca^+ Concentration

To directly alter Ca^{2+} entry during depolarization, and thereby affect any Ca^{2+}-dependent inactivation process, Ca^{2+} currents were studied with either 0.5 or 5 mM Ca^{2+} in the bath solution. When switching from 0.5 to 5 mM extracellular Ca^{2+}, the

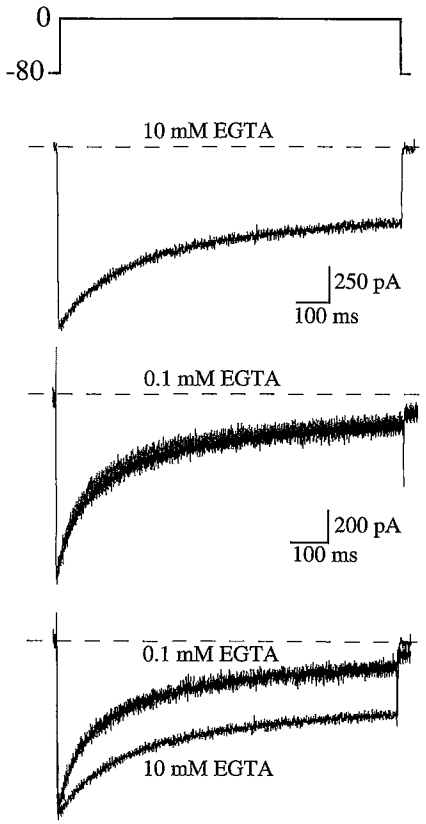

FIGURE 4. Effects of changing the intracellular Ca^{2+} buffer concentration. Ca^{2+} currents recorded from two separate cells with either 10 mM (*top*) or 0.1 mM (*middle*) EGTA in the patch pipette. The current in 10 mM EGTA was scaled to peak current in 0.1 mM EGTA and the two traces superimposed for comparison (*bottom*). In the middle panel, two consecutive traces are displayed. The gray colored trace was recorded 6 s after the darker trace. Traces recorded after current block with 5 μM ω-CgTx were used for leakage subtraction.

Ca^{2+} current measured with voltage steps from −80 to 0 mV increased from 2.3 to 4.1 fold (mean = 3.1 ± 0.51 fold; n = 15; Fig. 5, *upper panels*). With 0.1 mM EGTA in the internal solution, this increase in Ca^{2+} current caused a 40 ± 17% increase in the extent of inactivation measured at 200 ms, and a 29 ± 11% increase measured at 1 s (n = 7; Fig. 5 *A*). Furthermore, the rapid phase of inactivation became more prominent relative to the slow phase, such that the ratio of their amplitudes (A_{fast}/A_{slow}) increased from 0.7 to 1.9. The increase in rapid to slow inactivation observed in the presence of 0.1 mM EGTA was reversible after removal of the 5 mM

Ca^{2+}. The N current amplitude returned to control levels within 60 s after application of 5 mM Ca^{2+}. At this time, the ratio of fast to slow inactivation had recovered to 1.05, a value somewhat higher than that measured before application of high Ca^{2+}, but considerably lower than 1.9 the value observed with 5 mM external Ca^{2+}.

With 10 mM EGTA in the internal solution, the results were more complex. Eight experiments were performed in the same manner a that of Fig. 5 *A*, excepting that 10 mM rather than 0.1 mM EGTA was included in the patch pipette. In these experiments, a ~threefold increase in current amplitude had little effect on the kinetics of inactivation ($n = 8$; Fig. 5 *B*) suggesting that under these conditions inactivation is not significantly current dependent.

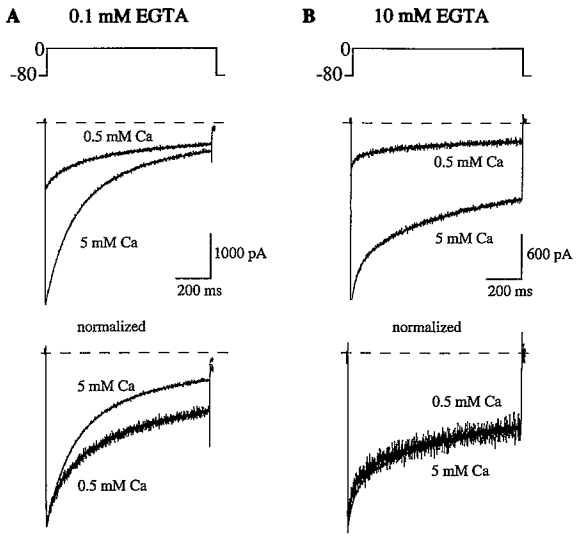

FIGURE 5. Effects of increasing the extracellular Ca^{2+} concentration. (*A*) Whole cell Ca^{2+} currents recorded during 1-s voltage steps from −80 to 0 mV with 0.1 mM EGTA in the patch pipette solution. The top panel shows current traces recorded with either 0.5 or 5 mM Ca^{2+} in the solution bathing the cell. These currents are normalized to their peaks and superimposed in the lower panel for comparison. (*B*) Shows the same experiment as in *A* performed on a different cell except that 10 mM rather than 0.1 mM EGTA was included in the patch pipette. Current traces were leakage subtracted using traces recorded following application of 5 μM ω-CgTx. (Solutions) External solutions contained (in millimolar): Na-glutamate 71, glutamic acid 70, TEA-OH 50, Hepes 25, CsOH 8.3, glucose 5, $MgCl_2$ 0.8, tetrodotoxin (TTx) 3 μM, and Ca-gluconate 5 (5 mM Ca) or Ca-gluconate 0.5 and Na gluconate 9 (0.5 mM Ca).

Experiments were also performed in which cells were held at −40 mV (10 mM internal EGTA) and the concentration of extracellular Ca^{2+} was elevated from 1 to 10 mM. If the loss of the rapid phase of inactivation normally observed upon depolarizing the holding potential from −80 to −40 mV (Fig. 2 *A*) is due to reduced Ca^{2+} influx during currents elicited from the more depolarized holding potential, then one would expect to recover the rapid phase of inactivation by increasing the amplitude of the currents elicited from −40 mV to the level observed with depolarizations from −80 mV. To test this, we performed the experiment illustrated in Fig. 6. Cells were held at −80 mV, and calcium currents were recorded at 0 mV in an extracellular solution containing 1 mM Ca^{2+} (trace *1*). The holding potential was then depolarized to −40 mV, and after 50–60 s, a smaller current with diminished rapid phase inactivation was observed (trace *2*). The cell was then superfused with a

solution which contained 10 mM Ca^{2+} and currents recorded (trace *3*). In seven such experiments, increases in current amplitude between 1.21 to 3.4 fold (mean = 2.2-fold) were observed when superfusing with 10 mM Ca^{2+}. In these cells, we saw little effect of the increase in current amplitude on the inactivation kinetics of the Ca^{2+} current. Before superfusion with 10 mM Ca^{2+}, the current recorded from a −40 mV holding potential inactivated to 89.6 ± 7.2% of peak in 200 ms and to 74.6 ± 8.6%

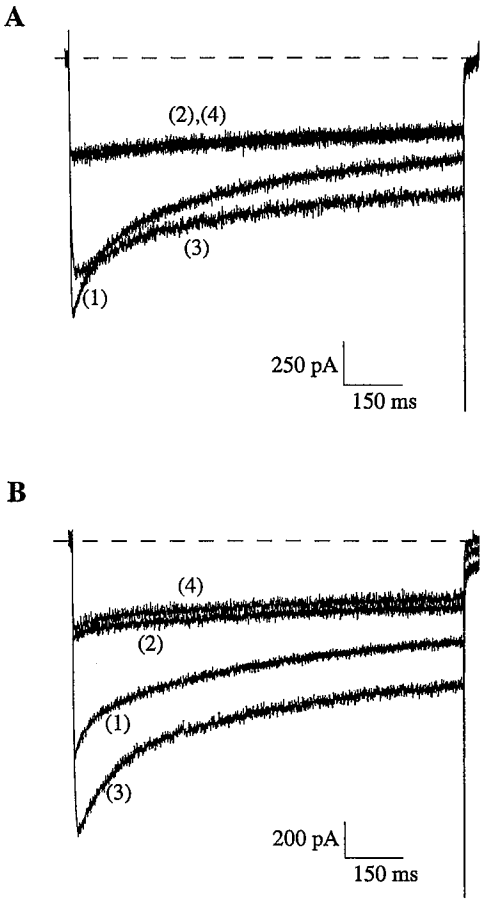

FIGURE 6. Effect of raising extracellular Ca^{2+} on currents elicited from a depolarized holding potential. Cells were bathed in a solution which contained 1 mM Ca^{2+}. Ca^{2+} currents were recorded from a holding potential of −80 mV (*1*). The holding potential was then depolarized to −40 mV and 50 s later, currents marked (*2*) were recorded. Cells were then superfused with a solution which contained 10 mM Ca^{2+} and the currents marked (*3*) were recorded. All test depolarizations were to 0 mV for 1 s. Capacity and leak currents were not subtracted from the current traces displayed. (*A*) An example of a cell in which superfusion with 10 mM Ca^{2+} (*3*) produced a 2.3-fold increase in current amplitude that had little effect on the inactivation of the current recorded from a −40 mV holding potential. The recovery trace (*4*) was recorded 170 s after superfusion was terminated. (*B*) An example of a cell which displayed a larger increase in current amplitude (3.5 fold) upon superfusion with 10 mM Ca^{2+} and the restoration of the rapid phase of inactivation. The recovery trace marked (*4*) was recorded 80 s after superfusion was terminated. (Solutions) External solutions contained (in millimolar): Na-glutamate 70–75, glutamic acid 50, TEA-OH 50, Hepes 25, CsOH 8.3, glucose 5, $MgCl_2$ 0.8, tetrodotoxin (TTx) 3 μM, and either Ca-gluconate 10, or Ca gluconate 1 and Na gluconate 18.

after 1 s. After the increase in extracellular Ca^{2+}, the larger current inactivated similarly to 88.0 ± 6.3% of peak in 200 ms and to 73.3 ± 10.3% after 1 s. In four of these seven cells, the current in 10 mM Ca^{2+} (−40 mV holding potential) was significantly smaller than the current measured in 1 mM Ca^{2+} (−80 mV holding potential); as a result, comparison of the inactivation kinetics of these currents was difficult to interpret. In three of these cells, however, the current in 10 mM Ca^{2+}

(−40 mV holding potential) was similar to that measured in 1 mM Ca^{2+} (−80 mV holding potential). One such experiment is shown in Fig. 6*A*. In this case, superfusing with 10 mM Ca^{2+} caused a 2.3-fold increase in current amplitude bringing the current measured from a −40 mV holding potential (trace *3*) near to the amplitude of the current measured from a −80 mV holding potential with 1 mM external Ca^{2+} (trace *1*). Despite the similarity in current amplitude the rapid phase of inactivation observed in trace *1* is not prominent in trace *3* indicating that with 10 mM EGTA in the internal solution current amplitude alone does not dictate Ca^{2+} current inactivation kinetics.

In four cells, however, when the amplitude of the Ca^{2+} current recorded from a −40 mV holding potential was increased by superfusing the cell with 10 mM Ca^{2+}, a prominent rapid phase of inactivation was observed. An example of one such experiment is shown in Fig. 6*B*. In this cell the peak amplitude of trace *3*, recorded in 10 mM external Ca^{2+} from a −40 mV holding potential, is 3.5-fold larger than that measured from the same holding potential with 1 mM external Ca^{2+} (trace *2*), and a rapid phase of inactivation now appears which is similar to that observed with pulses from −80 to 0 mV in 1 mM external Ca^{2+} (trace *1*). In the four cells which developed a rapid phase of inactivation the increase in current amplitude upon

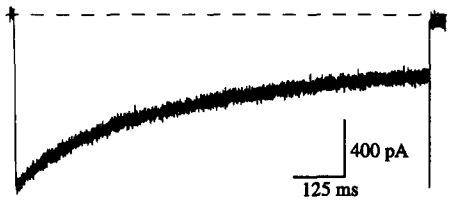

FIGURE 7. N channel current recorded with 5 mM BAPTA in the patch pipette and an extracellular solution containing 1 mM Ba^{2+}. Holding potential −80 mV; test potential 0 mV for 1 s.

perfusion with 10 mM Ca^{2+} was larger (3.5- to 4.8-fold; mean = 4.1) than in the seven experiments in which little change in kinetics was observed. In these experiments, the enhanced current inactivated to 71.3 ± 2.8% of peak in 200 ms and to 46.7 ± 8.4% after 1 s. In 1 mM Ca^{2+}, the smaller currents elicited from these same cells (held at −40 mV) inactivated to 85.3 ± 7.3% of peak in 200 ms and to 73.8 ± 12.6% after 1 s. It thus appears that increases in current amplitude of ~threefold or less are not sufficient to cause the appearance of the rapid phase of inactivation, however larger current increases do have significant effects on inactivation kinetics suggesting that, even with 10 mM EGTA as an intracellular Ca^{2+} buffer, large increases in Ca^{2+} influx can affect inactivation kinetics.

Some experiments were performed with BAPTA rather than EGTA included in the patch pipette solution. At physiological pH BAPTA has a similar affinity for Ca^{2+} as does EGTA but an on rate two to three orders of magnitude faster (Tsien, 1980). BAPTA should therefore more effectively buffer rapid Ca^{2+} transients occurring inside the cell. As with EGTA, with 5 mM intracellular BAPTA the ratio of rapid to slow inactivation was variable. In several cells, with depolarizations from −80 to 0 mV, both rapid and slow phases of inactivation were observed, even when Ba^{2+} was used as the charge carrier (Fig. 7). This further suggests that the rapid component of

inactivation observed with high concentrations of EGTA or BAPTA in the patch electrode is not entirely a current-dependent process.

N Current Carried by Na^+

To examine N current inactivation under conditions in which the current carrying ion was not likely to support Ca-dependent processes we studied N current carried predominately by Na^+ ions. As previously reported for L-type (Hess, Lansman, and Tsien, 1986) and N-type channels (Carbone and Lux, 1988; Jones and Marks, 1989), we found that the ω-CgTx-sensitive channels of chick DRG neurons became significantly permeant to monovalent cations when the extracellular Ca^{2+} concentration was reduced below micromolar levels. When no divalent cations were added to the extracellular solution and 1 mM EGTA was included, a sustained inward current was observed upon depolarization to potentials more positive than −55 mV. This current was predominately carried by Na^+ as evidenced by the fact that its amplitude was sensitive to the extracellular Na^+ concentration (usually set to 30 mM), and it was eliminated when Na^+ was eliminated from the bath solution (data not shown).

This current was inhibited by ω-CgTx. When cells were bathed in a low-divalent-cation solution and superfused with ω-CgTx (10 μM), Na^+ current through the N channels was eliminated ($n = 4$; Fig. 8 *A*). Although ω-CgTx-suppressed currents were not studied for an extended period of time, the block persisted after washout of ω-CgTx. (The longest time tested was 76 s.) Sensitivity to ω-CgTx was somewhat reduced when the experiment was performed in a different manner. When ω-CgTx was applied to the cells in a calcium-containing bath (which eliminated Ca^{2+} currents) and then a low-divalent-cation solution applied, some Na^+ current was observed in two of three cells tested. When compared to the amplitude of Na^+ currents measured in these cells before application of ω-CgTx, 13 and 35% of the current remained in the two cells (Fig. 8 *B*). Complete block was observed in the third cell. It appears, therefore, that ω-CgTx may be more effective against N current carried by Na^+ when the toxin is applied in the absence of Ca^{2+} (Carbone and Lux, 1988).

The variability in the degree of block by ω-CgTx might be taken as evidence for multiple channel types underlying this current. However, if multiple classes of channel exist, they must all fall into the pharmacological category of ω-CgTx-sensitive N-type channels, since all Ca^{2+} current was irreversibly blocked by the toxin (even in the two cells which exhibited residual Na^+ current). In any event, considering the complete block of Ca^{2+} current in these cells by ω-CgTx, it is likely that the sustained inward Na^+ current we have observed (measured in the presence of tetrodotoxin and the absence of significant external divalent cations) is passing through N channels.

Interestingly, the deactivation kinetics of Na^+ current through N channels (Fig. 9 *A*) often appeared slower than that of Ca^{2+} current. (Ca^{2+} current deactivation was fit with 1 exponential with a time constant of 430 μs; Na^+ current deactivation could be fit with two exponentials of time constants 0.67 and 5.4 ms.) This indicates that N channels have a longer mean open time, or reopen more frequently after repolarization with Na^+ rather than with Ca^{2+} as the current carrying ion.

Steady state activation curves (Fig. 9 *C*) for N current carried by either Ca^{2+} or Na^+ were determined by measuring the amplitude of tail currents upon repolarization to

the holding potential after step depolarizations to a series of test potentials. With Na^+ as the charge carrier the steady state activation curve was very similar in shape to that measured with Ca^{2+}. Both curves were fit by a Boltzmann equation with a slope factor of 6. The activation curve for Na^+, however, was shifted −15 mV relative to that for Ca^{2+}. This is most likely due to a surface charge effect resulting from the lowered extracellular divalent cation concentration (Hille, Woodhull, and Shapiro, 1975), because the Na^+ activation curve could be shifted to the position of the Ca^{2+} curve when 5 mM Mg^{2+} was added to the external solution (Fig. 9 *C*).

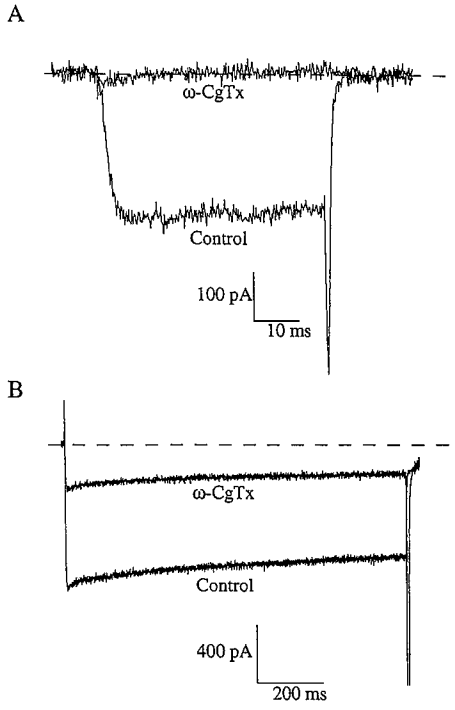

FIGURE 8. ω-CgTx-sensitivity of inward currents carried by Na^+ ions. Currents through Ca^{2+} channels carried by Na^+ recorded before (*control*), and after (*ω-CgTx*) application of ω-CgTx. (*A*) The cell was bathed in a low-divalent cation solution containing 20 mM Na^+. The control current was recorded, and the cell was then superfused for 30 s with 10 μM ω-CgTx dissolved in the same bath solution. The trace marked ω-CgTx was recorded ~30 s after the application of ω-CgTx was terminated (holding potential −80 mV, test potential −30 mV). (*B*) The bath solution contained 1 mM Ca^{2+}. The cell was superfused with a low-divalent cation solution containing 30 mM Na^+ and the control current was recorded. After washout of the low-divalent-cation solution, the cell was then superfused for 50 s with 5 μM ω-CgTx dissolved in the 1 mM Ca^{2+} bath solution. The cell was again superfused with the low-divalent cation solution and the trace marked ω-CgTx was recorded. This trace was recorded ~220 s after the termination of ω-CgTx application (holding potential −95 mV, test potential −25 mV). (*A*) Capacity and leak currents were subtracted using a P/4 protocol. Capacity and leak currents were not subtracted from the traces in *B*. Solutions (in millimolar): (*A*) bath: NMG-Cl 82.5, TEA-Cl 50, Hepes 25, NaCl 20, glucose 5, EGTA 1, TTx 0.3 μM; internal: NMG-Cl 155, Hepes 10, TEA-Cl 5, BAPTA 5. (*B*) bath: NMG-Cl 70, TEA-Cl 50, NaCl 30, Hepes 25, Glucose 5, $CaCl_2$ 1, $MgCl_2$ 0.8, TTX 3 μM; low-divalent-cation: NMG-Cl 72.5, TEA-Cl 50, NaCl 30, Hepes 25, Glucose 5, EGTA 1, TTx 3 μM; internal: NMG-Cl 154, Hepes 10, EGTA 10, NaCl 3.6.

To directly test for the involvement of Ca^{2+} in the inactivation process, currents through N channels carried by either Na^+ or Ca^{2+} were compared. To compensate for surface charge effects, N currents carried by Na^+ were compared to Ca^{2+} currents measured at potentials 15 mV more positive. Fig. 9 *B* shows current measurements taken before (Ca) and after (Na) removal of divalent cations from the extracellular solution. 10 mM EGTA was included in the patch pipette. The current carried by

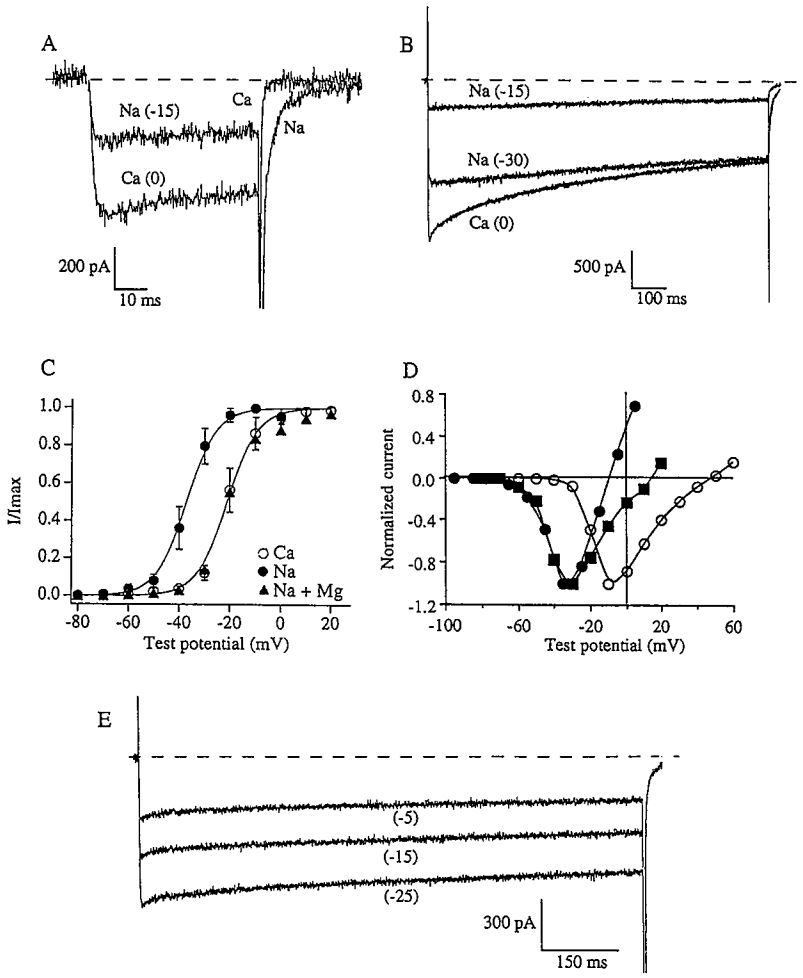

FIGURE 9. Na^+ current through N channels. (*A* and *B*) Currents in the presence of 1 mM external Ca^{2+} (Ca) or during superfusion with a Ca^{2+} free solution containing 1 mM EGTA and 30 mM Na^+ (Na). Holding potentials were −80 mV (Ca) and −95 mV (Na). Test potentials indicated in parentheses. Voltage steps were 50 ms in duration in *A* and 1 s in *B*. (*C*) Activation curves for N current carried by Ca^{2+} (○), Na^+ (●), and Na^+ in the presence of 5 mM extracellular Mg^{2+} (▲) were determined from tail current amplitudes measured at −80 mV after 50 ms depolarizations. Mean peak tail current amplitudes equaled 4421 ± 1682 pA (Ca), 1368 ± 660 pA (Na), 1047 ± 524 pA (Na + Mg). Points represent the mean ± SD of 10 (○), 6 (●), and 3 (▲) experiments. Data are fit with Boltzmann relations ($I/I_{max} = 1/(1 + \exp\{(V_{1/2} - V)/r\})$), $r = 6$, $V_{1/2} = -21$ (Ca and Na + Mg), $V_{1/2} = -37$ (Na). (*D*) Current-voltage curves normalized to peak current for N current carried by Ca^{2+} (with Cs^+ as the major intracellular cation, ○), Na^+ (with Cs^+ as the major intracellular cation, ●), and Na^+ (with NMG^+ as the major intracellular cation, ■). (*E*) N currents carried by Na^+ recorded during 1-s depolarizations to the indicated potentials from a holding potential of −95 mV (Cs^+ was replaced with NMG^+ as the major intracellular cation). (*A*, *C*, *D*) Capacity and leak currents were subtracted from the current records using a P/4 protocol from a holding potential of −100 (Ca) or −120 (Na). (*B*, *E*) Capacity and leak currents not subtracted. During exposure to

Ca^{2+} inactivated in a biphasic manner as already described. Na^+ current measured at an equivalent potential [Na(−15)], however, inactivated more slowly and in an approximately linear fashion. The loss of the rapid phase of inactivation when switching from Ca^{2+} to Na^+ was not due to differences in current amplitude as Na^+ currents measured as −30 mV (which were comparable in amplitude to Ca^{2+} currents measured at 0 mV) also exhibited only slow, monophasic inactivation [Na(−30)].

The smaller amplitude of the inward current carried by Na^+ compared to Ca^{2+} in Fig. 9, *A* and *B*, is likely not due to a decrease in the conductance of the N channels when divalent cations are reduced below micromolar levels, but rather to an increase in the permeability of the channels to Cs^+. Taking into account a 15 mV surface charge effect, this increase in Cs^+ permeability results in a −55 mV shift in the N current reversal potential from 60 mV (when Ca^{2+} carries the current) to 5 mV (when Na^+ carries the current) (Fig. 9 *D*). From calculations using the Goldman-Hodgkin-Katz current equation (Hille, 1992) the permeability ratio (P_{Cs}/P_{Na}) was determined to be (0.24) for N channels under conditions of low extracellular divalent cation concentration.

To better study the inactivation kinetics of inward Na^+ currents through N channels, internal Cs^+ was replaced with the less permeant ion *N*-methyl D-glucamine (NMG^+). When this was done, Na^+ currents measured at −15 mV with 30 mM extracellular Na^+ were similar in amplitude to Ca^{2+} currents recorded at 0 mV with 1 mM extracellular Ca^{2+}, and the current-voltage relation for Na^+ current through N channels reversed at 20 mV (Fig. 8 *D*). Although in two experiments, a slight component of fast inactivation was observed, in general Na^+ currents inactivated only slowly and in an approximately linear manner (Fig. 9 *E*). In 10 experiments, test pulses to −15 mV elicited Na^+ currents which inactivated to 11.1 ± 3.9% of peak in 200 ms and to 27.1 ± 7.8% in 1 s.

Inactivation of Ca^{2+} current as a function of prepulse potential reaches a maximum at the point of peak inward current, as expected for a Ca^{2+}-dependent process (Fig. 3). While it initially appeared that the U-shaped inactivation curve of Fig. 3 might be due in part to a Ca-dependent process, results of Fig. 5 *B* suggest that, with 10 mM internal EGTA, the changes in current amplitude observed over the middle of the voltage range tested are not likely to be sufficient to cause appreciable differences in inactivation rate, and therefore, that the U-shaped inactivation vs voltage relationship is more likely due to complex voltage-dependent inactivation. If this is the case,

---

solutions which contained low divalent cation concentrations, tight seals were often hard to maintain for more than 3 to 4 min. (Solutions) In *A* and *B*, the external solution for Ca^{2+} current measurement was identical to that used to measure Na^+ current (see Methods) except that 1 mM EGTA was replaced with 1 mM $CaCl_2$. For the experiments illustrated in *C, D,* and *E* for which Cs^+ was replaced with NMG^+ in the internal solution, the following internal and external solutions were used: internal, NMG-Cl 154–155, Hepes 10, EGTA 10 (*E*), or BAPTA 5(*C* and *D*), NaCl 3.6 (*E*) or TEA-Cl 5 (*C* and *D*). Calcium external: NaCl 93, NaOH 12.5, TEA-OH 50, Hepes 25, glucose 5, $CaCl_2$ 1, $MgCl_2$ 0.8, TTx 0.3 μM. Sodium external: NMG-Cl 82.5 (*C* and *D*) 72.5 (*E*), TEA-Cl 50, NaCl 20 (*C* and *D*) 30 (*E*), Hepes 25, glucose 5, EGTA 1, TTx 0.3 μM (*C* and *D*) 3 μM (*E*). For the Mg^{2+} shift experiment of 7C, 5 mM Mg^{2+} was added to this external solution and NMG-Cl was replaced with NaCl 75, NaOH 10.

then one would expect to see the same sort of U-shaped inactivation curve as is illustrated in Fig. 3 when Ca^{2+} is replaced with Na^+ as the charge carrying ion. Results of such an experiment are shown in Fig. 10. As seen in Fig. 10 *A*, 500 ms conditioning pulses to −55 mV (equivalent to a conditioning pulse to −40 mV in Ca^{2+}) produced little inward current. However, as judged by the ratio of current amplitudes measured during test pulses to −25 mV before and after the conditioning

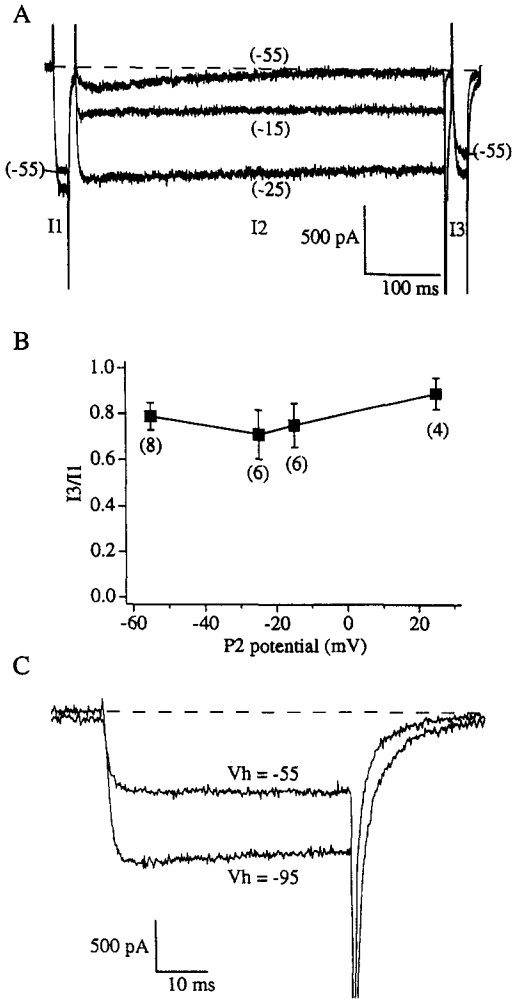

FIGURE 10. Na^+ current inactivation as a function of conditioning pulse potential. (*A*) The relationship between inactivation and conditioning pulse potential was studied for currents carried by Na^+ through N channels using the triple-pulse voltage protocol of Fig. 4. Holding potential was −95 mV. Test potentials (P1 and P2) were to −30 mV for 20 ms. Conditioning pulses were to −55, −25, −15, 25 (not displayed) mV for 500 ms. (*B*) The ratio I3/I1 is plotted as a function of conditioning pulse potential. Each point represents mean ± SD. The number of experiments for each point is indicated in parentheses. (*C*) N currents carried by Na^+ were recorded from a holding potential of −95 and after depolarization of the holding potential to −55 mV. Current traces in *C* were leakage subtracted using a P/4 protocol from a holding potential of −95 mV; those in *A* were not leakage subtracted.

pulse, they did produce a ~20% inactivation of the N current, an amount equal to that observed with depolarizations to −40 mV when Ca^{2+} was the charge carrying ion. However, with Na^+ as the charge carrier depolarizations to more positive potentials did not produce the same U-shape inactivation curve as was seen with Ca^{2+}. With conditioning-pulses to −55, −25, or −15 mV, the percent inactivation observed over 500 ms remained fairly constant, independent of current amplitude

(Fig. 10, *A* and *B*). With conditioning pulses to 25 mV, inactivation was somewhat less (~10%). These results suggest that the inactivation-voltage relation of Fig. 3 is in some sense Ca-dependent in that replacing Ca^{2+} with Na^+ alters the shape of the curve. Whether this Ca dependence arises from the absence of Ca^{2+} influx, or the removal of extracellular Ca^{2+} is not yet clear. The origin of the small transient current component sometimes observed with prepulses to −55 mV is unknown; however, as these traces were not leak subtracted with ω-CgTx, this component may represent a LVA current whose amplitude has been enhanced by the switch from Ca^{2+} to Na^+ as the charge carrier.

As with Ca^{2+} currents, Na^+ currents through N channels were also sensitive to the holding potential. When Na^+ currents were measured after prolonged depolarization of the holding potential from −95 to −55 mV, voltage-dependent inactivation produced a 50% reduction in current amplitude (Fig. 10 *C*).

DISCUSSION

The purpose of this study was to investigate the mechanisms behind the biphasic kinetics and holding-potential-dependence of N current inactivation. We found that the HVA Ca^{2+} current of chick DRG neurons inactivates in a biphasic manner, and that the rapid phase of inactivation is diminished relative to the slow phase when the holding potential from which currents are elicited is depolarized, as others have reported previously (Nowycky et al., 1985; Fox et al., 1987*a;* Swandulla and Armstrong, 1988). These kinetics cannot be ascribed to the presence of N- and L-type channels as originally suggested (Nowycky et al., 1985) because our studies were confined to ω-CgTx-sensitive, N-type current (Kasai, Aosaki, and Fukuda, 1987; McCleskey, Fox, Feldman, Cruz, Olivera, Tsien, and Yoshikami, 1987; Plummer et al., 1989; Swandulla et al., 1991). Similar inactivation properties have been observed for the N current of rat sympathetic (Plummer et al., 1989), rat DRG (Regan et al., 1991), and frog sympathetic neurons (Jones and Marks, 1989).

We have considered two models to explain the properties of N current inactivation in chick DRG neurons. First, that it is due to a combination of fast and slow, voltage-dependent processes, the fast component being incomplete even with strong depolarizations. The reduction in the ratio of rapid to slow inactivation upon depolarization of the holding potential could then be explained as follows. At depolarized holding potentials, a larger fraction of Ca^{2+} channels would be in an inactivated state, not available for opening. Fewer channels passing through the open state upon depolarization to 0 mV then would result in a smaller current relaxation to the new steady state level at which point only slow inactivation would be observed. In the second model, the N current inactivates by both slow, voltage-dependent and Ca-dependent mechanisms. In this model, depolarization of the holding potential inactivates a large fraction of channels due to voltage-dependent inactivation resulting in a smaller current upon depolarization to 0 mV. The reduced rate of Ca^{2+} influx would then result in a slower rate of Ca-dependent inactivation reducing the fast phase of inactivation.

Our experiments have produced three lines of evidence which indicate that the N current in chick DRG neurons can inactivate in Ca-dependent manner. Perhaps the strongest evidence comes from the observation that when the concentration of EGTA

in the patch pipette is lowered from 10 to 0.1 mM, the rapid phase of inactivation increased ~twofold relative to the slow phase, and the extent of inactivation in 1 s increased from 54 to 80% (Figs. 5 and 6). The changes in inactivation kinetics observed are likely due to a Ca^{2+}-dependent process. We considered as a potential source of artifact the possibility that in the low EGTA condition Ca^{2+} accumulated to such an extent near the intracellular face of the channels that the electrochemical driving force for current through the channels decreased over time. While we were not able to directly measure the Ca^{2+} concentration near the membrane, our simulations indicate that with 0.1 mM intracellular EGTA, over the course of a one second voltage step, the Ca^{2+} concentration near the membrane is not likely to rise to more than 35 μM. Even for internal concentrations as high 100 μM, however, calculations based on the mean field theory (Hagiwara, Ozawa and Sand, 1975) predict (with 5 mM extracellular Ca^{2+}) only a 2% reduction in current amplitude. Inactivation actually observed was 83% (Fig. 6). A change in driving force, therefore, is unlikely to contribute significantly to the increase in rate and extent of inactivation that we observed upon lowering the EGTA concentration in the patch pipette. More likely, there is an inactivation process which is Ca^{2+}-dependent, and the site at which Ca^{2+} acts is accessible by EGTA.

Further support for Ca^{2+}-dependent inactivation comes from the result that, with 0.1 mM EGTA in the patch pipette, increasing the Ca^{2+} current ~threefold by increasing the extracellular Ca^{2+} concentration significantly increased both the maximum amount inactivation and the ratio of the amplitude of the fast to the slow components. These effects are apparently due to a Ca-dependent process since each condition employed the same voltage protocol. We considered the possibility that the increase in the extent of inactivation observed when the extracellular Ca^{2+} concentration was increased was due to an effect on the surface charge of the membrane, effectively shifting the membrane potential in the negative direction 10 to 15 mV (Frankenhaeuser and Hodgkin, 1957; Hille et al., 1975). Results from Fig. 3, however, indicate that a shift in the test potential of this magnitude would have little effect on the extent of inactivation, while hyperpolarization of the holding potential over this range would be expected to have only a small influence ($< 10\%$) on the number of channels available for activation (Cox and Dunlap, 1992). After washout of the high Ca^{2+} solution, both current amplitude and inactivation kinetics recovered. Reversal of the inactivation kinetics lagged slightly behind that of current amplitude, however, suggesting a persistent effect of the high Ca^{2+} solution. Such an action may be related to a slow removal of intracellular Ca^{2+} that accumulated during pulses in the high Ca^{2+} solution.

A third line of evidence in support of current-dependent inactivation of N channels came from experiments using Na^+ as the permeant ion. Unlike Ca^{2+} currents, Na^+ currents through N channels did not exhibit a rapid phase of inactivation, decaying slowly and approximately linearly over the course of one second depolarizations. This observation also supports the conclusion that rapid inactivation is dependent on Ca^{2+} influx.

Not all data support the involvement of Ca^{2+} in fast-phase inactivation, however. Although high intracellular concentrations of EGTA or BAPTA (a more effective chelator, Kohr and Mody, 1991) reduced the fast phase component, they did not

eliminate it. Additionally, increases in current amplitude of ~threefold had little effect on the inactivation kinetics of N current under these conditions of high intracellular Ca^{2+} buffering. Finally, increases in peak Ca^{2+} current brought about by raising extracellular Ca^{2+} did not reverse the reduction in rapid inactivation produced by depolarizing holding potentials unless the increases in peak current were very large (>3.5-fold). The most reasonable explanation for this latter result is that when the rate of Ca^{2+} entry is greatly increased, the intracellular Ca^{2+} concentration is not effectively buffered by 10 mM EGTA, and the Ca-dependent inactivation process becomes manifest. Bechem and Pott (1985) reported similar results, demonstrating that 20 mM EGTA in the patch electrode was unable to completely suppress the Ca-dependent inactivation of Ca^{2+} current recorded from guinea-pig atrial myocytes. Thus, certain of our results are at odds with a strictly current-dependent inactivation model which predicts an increase in the ratio of fast to slow inactivation with an increase in the rate of Ca^{2+} entry (Eckert and Chad, 1984).

Although the Na^+-substitution experiments support current-dependent inactivation, the interpretation of the data might be complicated. It is possible that removal of external Ca^{2+} affects the gating of the N channels directly, in a manner unrelated to Ca^{2+} entry. In support of this idea, the deactivation kinetics of currents carried by Na^+ were found to be slower than those carried by Ca^{2+}, an effect which is likely due to destabilization of the closed state of the channel in the absence of external Ca^{2+} (Swandulla and Armstrong, 1989). The steady state activation curves of Fig. 9 *C* on the other hand, demonstrate that during short depolarizations the relation between the proportion of channels in an open state and membrane potential is not altered when switching from Ca^{2+} to Na^+ as the charge carrier. Other channels are known to be sensitive to extracellular Ca^{2+}, the rate of K^+ current inactivation in T lymphocytes, for example, has been reported to increase as the external Ca^{2+} concentration is raised (Grissmer and Cahalan, 1989). One final possibility to be explored in future experiments is that a subset of N channels, those which inactivate rapidly, do not pass monovalent ions and thus do not contribute to Na^+ current measurements.

We have also examined inactivation as a function of membrane potential. In two-pulse experiments with 10 mM internal EGTA and Ca^{2+} as the charge carrier (Fig. 3) the relationship between conditioning pulse potential and inactivation of Ca^{2+} current during the test pulse has a concave upward, U shape, with maximum inactivation occurring at the point of peak inward current. As originally demonstrated by Brehm et al. (1978), such a U shape is consistent with a current-dependent inactivation mechanism, and is inconsistent with a simple voltage-dependent mechanism with inactivating rate constants which increase with more positive depolarizations. Results of Fig. 5 *B*, however, indicate that with 10 mM EGTA in the patch pipette, the changes in current amplitude produced by varying the test potential in Fig. 3 are not likely to produce significant Ca-dependent inactivation. An alternative explanation is needed. In many respects our results are similar to Jones and Marks (1989) who studied the inactivation of ω-CgTx-sensitive Ca^{2+} current in bullfrog sympathetic neurons. Inactivation of this current proceeds with both fast and slow components. In two pulse experiments similar to that of Fig. 3 they also observed a U shaped relationship between prepulse potential and the extent of N current inactiva-

tion. They proposed that a U-shaped inactivation curve could be produced by a strictly voltage-dependent process in which the rate of inactivation decreased with more positive depolarizations. In their model, the negative slope of the inactivation-voltage curve at negative potentials is due to a region over which the microscopic rate constant for channel opening is increasing faster than the rate constant for inactivation is decreasing. Such a mechanism could account for the U-shaped inactivation curve we have observed, and therefore offers a reconciliation between the apparently contradictory results of Figs. 3 and 5 *B*. Lowering the concentration of Ca^{2+} chelator in the patch pipette did not have substantial effects upon the inactivation kinetics of the N current recorded from bullfrog sympathetic neurons, thereby distinguishing the results of Jones and Marks (1989) from those reported here. It appears, therefore, that among channels which conform to the pharmacological definition of N-type, there are subtypes with differing sensitivity to intracellular Ca^{2+}.

The ability of 10 mM EGTA to suppress the Ca-dependent component of inactivation we have observed suggests that the site of Ca^{2+} action may be some distance away from the channel protein as the extent to which EGTA effectively buffer intracellular Ca^{2+} declines precipitously within tens of nanometers of the channel pore (Gutnick, Lux, Swandulla, and Zucker, 1989). For the Ca^{2+} current of *Helix* neurons an enzymatic mechanism of Ca-dependent inactivation has been suggested whereby dephosphorylation of the channels by a Ca-dependent phosphatase causes channel inactivation (Chad and Eckert, 1986). If such a mechanism were operative for N channels, differences in the expression of regulatory proteins between cell types might also affect the extent to which Ca-dependent inactivation is observed. Clearly more investigation is necessary to determine if Ca^{2+} is acting in this system by an enzymatic pathway.

In summary, our results indicate that the inactivation of N current in chick DRG neurons is quite complex. With high concentrations of intracellular Ca^{2+} chelator our results are best explained by a combination of fast and slow voltage-dependent processes. When lower concentrations of EGTA are used in the patch pipette a current-dependent inactivation mechanism becomes apparent. While Ca-dependent inactivation is likely to be minimal under the whole cell recording conditions often used to study Ca^{2+} current, it may contribute substantially to inactivation in vivo.

Independent support for the presence of a Ca-dependent inactivation mechanism associated with the N-type Ca^{2+} channels of chick DRG neurons comes from the work of Morad, Davies, Kaplan, and Lux (1988). Using the photosensitive Ca^{2+} chelating agent DM-nitrophen they produced a rapid rise in the intracellular Ca^{2+} concentration of freshly dissociated chick DRG neurons and observed a rapid inhibition of HVA Ca^{2+} current. Because the great majority of HVA Ca^{2+} current in these cells is blocked by ω-CgTx, it is likely that the inactivation studied by Morad et al. (1988) was of N-type channels. Our studies are also consistent with those of Kasai and Aosaki (1988) who, also studying chick sensory neurons, reported an increase in the relative proportion of fast to slow inactivation when the concentration of EGTA was lowered in the patch pipette. Interestingly, in their experiments, Ba^{2+} was used as the charge carrier suggesting that Ba^{2+}, as well as Ca^{2+}, is able to support current-dependent inactivation.

It is perhaps not surprising that N channels exhibit Ca^{2+}-dependent inactivation. In addition to in a variety of invertebrate systems (Brehm and Eckert, 1978; Tillotson, 1979; Ashcroft and Stanfield, 1981; Eckert and Chad, 1984; Gutnick et al., 1989; Johnson and Byerly, 1993), Ca^{2+}-dependent inactivation has been described for L-type Ca^{2+} channels of mammalian cardiac muscle and neurohypophysis (Kass and Sanguinetti, 1984; Bechem and Pott, 1985; Kalman et al., 1988; Yue, Backx, and Imredy, 1990). Negative feedback control of Ca^{2+} entry may be a common mechanism for the regulation of intracellular Ca^{2+} levels. At nerve terminals, where N channels play a role in neurosecretion, adaptive responses to a series of stimuli might be due, in part, to the inactivation of Ca^{2+} channels as the intraterminal Ca^{2+} concentration rises with each successive stimulus (Klein, Shapiro, and Kandel, 1980; Nowycky, 1991) as well as to the more rapid phase of voltage-dependent inactivation. Voltage-dependent inactivation of N channels might also play a role in presynaptic inhibition caused by prolonged subthreshold depolarizations as is produced in primary afferent nerve terminals of the spinal cord in response to repetitive stimulation (Frank and Fourtes, 1957; Eide et al., 1968).

This work was supported by United States Public Health Services grant NS16483.

Original version received 15 April 1993 and accepted version received 31 January 1994.

REFERENCES

Aosaki, N., and H. Kasai. 1989. Characterization of two kinds of high-voltage-activated Ca-channel currents in chick sensory neurons. Differential sensitivity to dihydropyridines and omega-conotoxin GVIA. *Pflügers Archiv.* 414:150–156.

Ashcroft, F. M., and P. R. Stanfield. 1981. Calcium dependence of the inactivation of calcium currents in skeletal muscle fibers of an insect. *Science.* 213:224–226.

Augustine, G. J., M. P. Charlton, and S. J. Smith. 1987. Calcium action in synaptic transmitter release. *Annual Review of Neuroscience.* 10:633–693.

Bechem, M., and L. Pott. 1985. Removal of Ca current inactivation in dialysed guinea-pig atrial cardioballs by Ca chelators. *Pflügers Archiv.* 404:10–20.

Bernheim, L., C. R. Bader, D. Bertrand, and R. Schlichter. 1989. Transient expression of Ca-activated Cl current in developing quail sensory neurons. *Developmental Biology.* 136:129–139.

Boland, L. M., and B. P. Bean. 1993. Modulation of N-type calcium channels in bullfrog sympathetic neurons by luteinizing hormone-releasing hormone: kinetics and voltage dependence. *Journal of Neuroscience.* 13:516–533.

Brehm, P., and R. Eckert. 1978. Calcium entry leads to inactivation of calcium channel in *Paramecium*. *Science.* 202:1203–1206.

Carbone, W., and H. D. Lux. 1988. ω-conotoxin blockade distinguishes Ca from Na permeable states in neuronal calcium channels. *Pflügers Archiv.* 413:14–22.

Catterall, W. A. 1991. Excitation-contraction coupling in vertebrate skeletal muscle: a tale of two calcium channels. *Science.* 242:50–61.

Chad, J. E., R. Eckert, and D. Ewald. 1984. Kinetics of calcium-dependent inactivation of calcium current in voltage-clamped neurones of *Aplysia californica*. *Journal of Physiology.* 347:279–300.

Chad, J. E., and R. Eckert. 1986. An enzymatic mechanism for calcium current inactivation in dialysed helix neurones. *Journal of Physiology.* 378:31–51.

Cox, D. H., and K. Dunlap. 1992. Pharmacological discrimination of N-type from L-type calcium current and its selective modulation by transmitters. *Journal of Neuroscience.* 12:906–914.

Dunlap, K., and G. D. Fischbach. 1978. Neurotransmitters decrease the calcium component of sensory neurone action potentials. *Nature.* 276:837–389.

Dunlap, K., and G. D. Fischbach. 1981. Neurotransmitters decrease the calcium conductance activated by depolarization of embryonic chick sensory neurones. *Journal of Physiology.* 317:519–535.

Eckert, R., and J. E. Chad. 1984. Inactivation of Ca Channels. *Progress in Biophysics and Molecular Biology.* 44:215–267.

Eide, E., I. Jurna, J. Jansen, and A. Lunberg. 1968. Conductance measurements from motorneurons during presynaptic inhibition. *In* Structure and Function of Inhibitory Neuronal Mechanisms. Pergammon Press, London. 215–219.

Elmslie, K. S., W. Zhou, and S. W. Jones. 1990. LHRH and GTP-g-S modify calcium current activation in bullfrog sympathetic neurons. *Neuron.* 5:75–80.

Forscher, P., and G. S. Oxford. 1985. Modulation of calcium channels by norepinephrine in internally dialyzed avian sensory neurons. *Journal of General Physiology.* 85:743–763.

Fox, A. P., M. C. Nowycky, and R. W. Tsien. 1987*a*. Kinetics and pharmacological properties distinguishing three types of calcium currents in chick sensory neurones. *Journal of Physiology.* 394:149–172.

Fox, A. P., M. C. Nowycky, and R. W. Tsien. 1987*b*. Single-channel recordings of three types of calcium channels in chick sensory neurones. *Journal of Physiology.* 394:173–200.

Frank, K., and G. R. Fourtes. 1957. Presynaptic and postsynaptic inhibition of monosynaptic reflexes. *Federation Proceedings.* 16:39–40.

Frankenhaeuser, B., and A. L. Hodgkin. 1957. The action of Calcium on the electrical properties of squid axons. *Journal of Physiology.* 137:218–244.

Gutnick, M. J., H. D. Lux, D. Swandulla, and H. Zucker. 1989. Voltage-dependent and calcium-dependent inactivation of calcium channel current in identified snail neurones. *Journal of Physiology.* 412:197–220.

Grissmer, S., and M. D. Cahalan. 1989. Divalent ion trapping inside potassium channels of human T lymphocytes. *Journal of General Physiology.* 93:609–630.

Gruner, W., L. R. Silva, and K. Dunlap. 1992. ω-Conotoxin sensitive calcium current mediates presynaptic inhibition at the sensory neuron-spinal cord synapse. *Society for Neuroscience Abstracts.* 18:114.17. (Abstr.)

Hagiwara, S., S. Ozawa, and O. Sand. 1975. Voltage-clamp analysis of two inward current mechanisms in the egg cell membrane of a star fish. *Journal of General Physiology.* 63:564–578.

Hamill, O. P., A. Marty, E. Neher, B. Sakmann, and F. J. Sigworth. 1981. Improved patch-clamp techniques for high-resolution current recordings from cells and cell-free membrane patches. *Pflügers Archiv.* 391:85–100.

Hess, P., J. B. Lansman, and R. W. Tsien. 1986. Calcium channel selectivity for divalent and monovalent cations. Voltage and concentration dependence of single channel current in ventricular heart cells. *Journal of General Physiology.* 88:293–319.

Hille, B. 1992. Ionic Channels of Excitable Membranes. Sinauer Associates Inc, Sunderland, MA. 607 pp.

Hille, B., A. M. Woodhull, and B. I. Shapiro. 1975. Negative surface charge near sodium channels of nerve: divalent ions, monovalent ions, and pH. *Philosopical Transactions of the Royal Society, Series B.* 270:301–318.

Hirning, L. D., A. P. Fox, E. W. McCleskey, B. M. Olivera, S. A. Thayer, R. J. Miller, and R. W. Tsien. 1988. Dominant role of N-type Ca channels in evoked release of norepinephrine from sympathetic neurons. *Science.* 239:57–61.

Hodgkin, A. L., and A. F. Huxley. 1952. The dual effect of membrane potential on the sodium conductance in the giant axon of *Loligo*. *Journal of Physiology*. 116:497–506.

Holz, G. G., K. Dunlap, and R. M. Kream. 1988. Characterization of electrically-evoked release of substance P from dorsal root ganglion neurons: Methods and dihydropyridine sensitivity. *Journal of Neuroscience*. 8:463–471.

Horne, A. L., and J. A. Kemp. 1991. The effect of ω-conotoxin GVIA on synaptic transmission within the nucleus accumbens and hippocampus of the rat *in vitro*. *British Journal of Pharmacology*. 103:1733–1739.

Johnson, B. D., and L. Byerly. 1993. Photoreleased intracellular Ca^{2+} rapidly blocks Ba^{2+} current in *Lymnaea* neurons. *Journal of Physiology*. 462:321–347.

Jones, S. W., and T. N. Marks. 1989. Calcium currents in bullfrog sympathetic neurons. II. *Inactivation*. *Journal of General Physiology*. 94:169–182.

Kalman, D., P. H. O'Lague, C. Erxleben, and D. Armstrong. 1988. Calcium-dependent inactivation of the dihydropyridine-sensitive calcium channels in GH3 cells. *Journal of General Physiology*. 92:531–548.

Kasai, H., and T. Aosaki. 1988. Divalent cation-dependent inactivation of the high-voltage-activated Ca channel current in chick sensory neurons. *Pflügers Archiv*. 411:695–697.

Kasai, H., and T. Aosaki. 1989. Modulation of Ca-channel current by an adenosine analog mediated by a GTP-binding protein in chick sensory neurons. *Pflügers Archiv*. 414:145–149.

Kasai, H., T. Aosaki, and J. Fukuda. 1987. Presynaptic Ca-antagonist ω-conotoxin irreversibly blocks N-type Ca-channels in chick sensory neurons. *Neuroscience Research*. 4:228–235.

Kass, R. S., and M. C. Sanguinetti. 1984. Inactivation of calcium current in the calf cardiac Purkinje fiber: evidence for voltage and calcium-mediated-mechanisms. *Journal of General Physiology*. 84:705–26.

Kerr, L. M., and D. Yoshikami. 1984. A venom peptide with a novel presynaptic blocking action. *Nature*. 308:282–284.

Klein, M., E. Shapiro, and E. R. Kandel. 1980. Synaptic plasticity and the modulation of the Ca current. *Journal of Experimental Biology*. 89:117–157.

Kohr, G., and I. Mody. 1991. Endogenous intracellular calcium buffering and activation/inactivation of HVA calcium current in rat dente gyrus granule cells. *Journal of General Physiology*. 98:941–967.

Lipscombe, D., S. Kongsamut, and R. W. Tsien. 1989. α-Adrenergic inhibition of sympathetic neurotransmitter release mediated by modulation of N-type calcium-channel gating. *Nature*. 340:639–642.

Llinas, R., M. Sugimori, D. E. Hillman, and B. Cherksey. 1992. Distribution and functional significance of the P-type Ca channels in the mammalian central nervous system. *Trends in Neuroscience*. 15:351–355.

Mayer, M. L. 1985. A calcium-activated chloride current generates the after-depolarization of rat sensory neurones in culture. *Journal of General Physiology*. 364:217–239.

McCleskey, E. W., A. P. Fox, D. H. Feldman, L. J. Cruz, B. M. Olivera, R. W. Tsien, and D. Yoshikami. 1987. ω-conotoxin: direct and persistent blockade of specific types of calcium channels in neurons but not muscle. *Proceedings of the National Academy of Sciences, USA*. 84:4327–4331.

Morad, M., N. W. Davies, J. H. Kaplan, and H. D. Lux. 1988. Inactivation and block of calcium channels by photo-released Ca^{2+} in dorsal root ganglion neurons. *Science*. 241:842–844.

Nowycky, M. C. 1991. Two high-threshold Ca channels contribute Ca for depolarization-secretion coupling in the mammalian neurohypophysis. *Annals of the New York Academy of Sciences*. 635:45–57.

Nowycky, M. C., A. P. Fox, and R. W. Tsien. 1985. Three types of neuron calcium channel with different calcium agonist sensitivity. *Nature*. 316:440–443.

Plummer, M. R., D. E. Logothetis, and P. Hess. 1989. Elementary properties and pharmacological sensitivities of calcium channels in mammalian peripheral neurons. *Neuron.* 2:1453–1463.

Rane, S. G., and K. Dunlap. 1990. G protein- and kinase C-mediated regulation of voltage-dependent calcium channels. *In* G Proteins. L. Birnbaumer and R. Iyengar, editors. Academic Press, San Diego, CA. 357–381.

Regan, L. J., D. W. Sah, and B. P. Bean. 1991. Ca channels in rat central and peripheral neurons: High-threshold current resistant to dihydropyridine blockers and ω-conotoxin. *Neuron.* 6:269–280.

Sah, D. W. 1990. Neurotransmitter modulation of calcium current in rat spinal cord neurons. *Journal of Neuroscience.* 10:136–141.

Sheng, M., G. McFadden, and M. E. Greenberg. 1990. Membrane depolarization and calcium induced c-fos transcription via phosphorylation of transcription factor CREB. *Neuron.* 4:571–582.

Swandulla, D., and C. M. Armstrong. 1988. Fast-deactivating Ca channels in chick sensory neurons. *Journal of General Physiology.* 92:197–218.

Swandulla, D., and C. M. Armstrong. 1989. Calcium channel block by cadmium in chicken sensory neurons. *Proceedings of the National Academy of Sciences, USA.* 86:1736–1740.

Swandulla, D., E. Carbone, and H. D. Lux. 1991. Do calcium channel classifications account for neuronal calcium channel diversity. *Trends in Neuroscience.* 14:46–51.

Tsien, R. Y. 1980. New Calcium indicators and buffers with high selectivity against magnesium and protons: design, synthesis, and properties of prototype structures. *Biochemistry.* 19:2396–2404.

Tillotson, D. 1979. Inactivation of Ca conductance dependent on entry of Ca ions in mulluscan neurons. *Proceedings of the National Academy of Sciences, USA.* 77:1497–1500.

Yue, D. T., P. B. Backx, and J. P. Imredy. 1990. Calcium-sensitive inactivation in the gating of single calcium channels. *Science.* 250:1735–1738.